Journal Pre-proof

Nanoparticles hydrothermal simulation in a pipe with insertion of compound turbulator analyzing entropy generation

Qiang Pu, M. Jafaryar, Samir Mustafa Hamad, Azeez A. Barzinjy, Ahmad Shafee, Elham Abohamzeh, Iskander Tlili

PII: S0378-4371(19)31714-5
DOI: https://doi.org/10.1016/j.physa.2019.123038
Reference: PHYSA 123038

To appear in: *Physica A*

Received date : 2 April 2019
Revised date : 25 July 2019

Please cite this article as: Q. Pu, M. Jafaryar, S.M. Hamad et al., Nanoparticles hydrothermal simulation in a pipe with insertion of compound turbulator analyzing entropy generation, *Physica A* (2019), doi: https://doi.org/10.1016/j.physa.2019.123038.

*Highlights (for review)

Highlights

- Irreversibility and heat transfer simulation for nanomaterial is scrutinized.
- Compound turbulator has been used to make secondary flow.
- $S_{gen,f}$ augments with augment of *Re*.
- Irreversibility due to heat transfer declines with augment of *b*

Nanoparticles hydrothermal simulation in a pipe with insertion of compound turbulator analyzing entropy generation

Qiang Pu [a], M. Jafaryar [b], Samir Mustafa Hamad [c,d], Azeez A. Barzinjy [e,f], Ahmad Shafee [g], Elham Abohamzeh [h], Iskander Tlili [1,i,j]

[a] *School of Information Science and Engineering, Chengdu University, Chengdu 610106, China*
[b] *Renewable energy systems and nanofluid applications in heat transfer Laboratory, Babol Noshirvani University of Technology, Babol, Iran*
[c] *Computer Department, Cihan University-Erbil, Iraq*
[d] *Scientific Research Centre, Soran University, Soran, Kurdistan Region, Iraq*
[e] *Physics Education Department, Tishk International University TIU, Erbil, Kurdistan Region – Iraq*
[f] *Physics Department, College of Education, Salahaddin University-Erbil, Kurdistan Region – Iraq*
[g] *Public Authority of Applied Education and Training, College of Technological Studies, Applied Science Department, Shuwaikh, Kuwait*
[h] *Department of Energy, Material and Energy Research Center (MERC), Karaj, Iran*
[i] *Department for Management of Science and Technology Development, Ton Duc Thang University, Ho Chi Minh City, Vietnam*
[j] *Faculty of Applied Sciences, Ton Duc Thang University, Ho Chi Minh City, Vietnam*

Abstract

The aim of this investigation is to investigate the H_2O turbulent flow according to the nanoparticles, including copper oxide within a pipe outfitted by an innovative swirling flow generator. For the purpose of determining width effect in turbulent flow for Reynolds number, the results are analyzed. Moreover, relationships are obtained to estimate the irreversibility component. It is observed that viscous reduces directly proportional to pumping power. This means that following an increase in inlet velocity, differential pressure rises. Because of higher velocity gradient, by increasing width $S_{gen,f}$ becomes greater. As turbulator with larger b is used, stronger turbulence intensity will be generated.

Keywords**:** Swirling flow generator; Nanomaterials; Thermal performance; Computational Fluid dynamic modeling; Entropy.

1. Introduction

[1] Corresponding author:
Email address: iskander.tlili@tdtu.edu.vn (Iskander Tlili)

Increasing energy consumption in recent decades, made scientists search on possible solutions to face this energy crisis. In this regard, developing a heat exchanger with a more inclusive efficiency and smaller dimension presents a suitable solution. Employing Swirling flow generator combined with nanotechnology could be regarded as an effective way.

Chio [1] was the first to propose the term "Nanofluid", which is suspension consisting of nano-sized powders (1-100mm) within a liquid medium. Comparing to base fluid, nanofluids have better thermo-physical characteristics which make them be regarded as future working fluids. Nanofluids can be used as a solution of a variety of industrial problems with comprehensive functions such as air conditioning, chilling of electronic instruments, heat pipes, heat exchangers, oil recovery, drug delivery appliances, diesel-electric generator, heating buildings, nano- lubricants of high-temperature pumps, and pollution reduction. In order to prove the ability of nanoparticle several papers were published [2-13]. Wu et al. [14] deduced $Al2O3 - H2$O nanofluid results in power penalty in pumping of micro duct. Increasing inlet speed and volume concentration of nanofluid leads to a quick boost of the mentioned penalty. Ahmed et al. [15] predicted a new model of a microchannel heat sink with two layers of aluminum in shapes of rectangle and triangle, with alumina and $SiO_2 - H_2O$ nanomaterial. Their conclusion determined that the alumina had the finest efficiency with two layered micro duct, in a triangle shape.

Wang et al. [16] analyzed the efficiency of heat pipes containing aqueous CuO nanomaterial as the heat transfer fluid. In the case of unsteady state, while the working fluid was aqueous CuO nanofluid, the startup time was declined. Heat transfer was improved considerably by 40% along with a 50% decline in thermal resistance was observed, in the cases which nanofluid was adopted as the working fluid, rather than utilizing D.I. water. To predict thermal behavior several methods can be utilized for simulation [17-32]. The heat transfer of four distinct nanoparticles, with various volume concnetration in trapezoidal plate heat exchangers, was assessed by Abed et al. [33]. The impact of dimensional factors of trapezoid channels was scrutinized. Based on the results, the largest Nusselt number is observed for SiO2. Improvement in the heat transfer took place with concentration. However, there was a minor rise in pressure loss along with the decline in nanoparticle diameter. There was also an augment in the Nu for nanoparticle having diameters of 20 nm. The heat transfer improvement was 35% more in comparison with water.

Forced convection under turbulent flow and friction of alumina nanomaterial, which flows in a U-bend tube, once with helical tape in the inlet tube, and another time without it, was scrutinized by Durga Prasad et al. [34]. They concluded that the rise in the Reynolds and Prandtl numbers cause increasing of Nu. Compared to water, an improvement of 32.91% in the Nu in whole pipes is observed for 0.03% concentration and p/d=5. The volume averaging procedure in order to figure out the Buongiorno model for nanomaterial forced convection inside a duct was applied by Zhang et al. [35]. They accomplished pore-scale scrutiny to illustrate thermal dispersion as well as mechanical dispersion. The detailed expression of the Nu for channel and tube flows for the analytical solution was demonstrated. Besides, another ways exist for augmentation in heat transfer [36-77]. Asmaie et al. [78] studied a thermosyphon with numerical analysis, by utilizing CuO /water nanofluid. The outcome illustrated that the efficient concentration to bring about the best heat transfer improvement was 1% wt. Furthermore, they recognized that by this concentration, it was feasible to acquire 46% excessive maximum heat flux when compared with water-filled thermo syphon. Xuan et al. [79] carried out research about solar energy absorption by applying unitary nanofluids of Ag and TiO2 as well as their hybrid. The results show that the hybrid nanofluid functioned properly and resulted in increased temperature in comparison with TiO_2. Furthermore, it's temperature was the same as Ag, nevertheless, the price of nanocomposite TiO_2/silver is lower. Accordingly, the research suggested utilizing nanocomposite rather than unitary nanoparticles.

Although there is much research in this area, the nanomaterial irreversibility in the pipe with a turbulator, which is the main goal of current research is studied in few publications. In current work, the behavior of working fluid in turbulent flow as the single phase one is investigated via a finite volume method.

2. Modeling Heating unit for the simulation

A view of the studied pipe which is fitted with turbulator is shown in Fig. 1. K-ε model, proving to be the best solution [80] was applied in this study. In order to reach a desired y+ value for this model, unstructured meshes with inflations on facades are used. Single-phase fluid with relation similar to [81] was implemented to reduce the computational cost. Selecting Mixture of nanoparticles and H2O is based on [81]. Moreover, in order to reduce the computational time and cost, single-phase fluid with relations such as [81] are implemented. To avoid further complexity, Gravity forces and heat loss can be neglected. The equation considering k-ε model is written as follows:

$$\frac{\partial (u_i)}{\partial x_i} = 0 \tag{1}$$

$$\frac{\partial}{\partial x_j}\left(\rho_{nf} u_i u_j\right) = -\frac{\partial p}{\partial x_i} + \frac{\partial}{\partial x_j}\left(\left(\frac{\partial u_i}{\partial x_j} + \frac{\partial u_j}{\partial x_i}\right)\mu_{nf}\right) + \frac{\partial}{\partial x_j}\left(-\rho_{nf}\, \overline{u_j' u_i'}\right) \tag{2}$$

$$\frac{\partial}{\partial x_i}\left(\rho_{nf} T u_i\right) = \frac{\partial}{\partial x_i}\left(\left(\Gamma + \Gamma_t\right)\frac{\partial T}{\partial x_i}\right), \quad \Gamma\left(=\mu_{nf} / \mathrm{Pr}_{nf}\right), \quad \Gamma_t\left(=\mu_t / \mathrm{Pr}_t\right) \tag{3}$$

the turbulent dissipation rates and kinetic energy are specified as follows:

$$-\rho_{nf}\overline{u_i' u_j'} = \left(\frac{\partial u_i}{\partial x_j} + \frac{\partial u_j}{\partial x_i}\right)\mu_t - \frac{2}{3}\rho_{nf} k \delta_{ij} - \frac{2}{3}\mu_t \frac{\partial u_k}{\partial x_k}\delta_{ij} \quad (4)$$

$$\mu_t = \frac{1}{\varepsilon} k^2 C_\mu \rho_{nf} \quad (5)$$

As previously mentioned, in the presence of turbulator in a pipe, k-ε model is regarded as the most precise model. Conceding the turbulent fluid model superimposed two scalars as follows:

$$\frac{\partial}{\partial x_j}\left(\left(\frac{\mu_t}{\sigma_k} + \mu_{nf}\right)\frac{\partial k}{\partial x_j}\right) - \rho_{nf}\varepsilon + G_k = \frac{\partial}{\partial x_i}\left(u_i \rho_{nf} k\right),\ G_k = -\rho_{nf}\overline{u_j' u_i'}\frac{\partial u_j}{\partial x_i} \quad (6)$$

$$\frac{\partial}{\partial x_i}\left(u_i \rho_{nf}\varepsilon\right) = \frac{\varepsilon}{k} G_k C_{1\varepsilon} - \rho_{nf}\frac{\varepsilon^2}{k} C_{2\varepsilon} + \frac{\partial}{\partial x_j}\left(\left(\frac{\mu_t}{\sigma_\varepsilon} + \mu_{nf}\right)\frac{\partial \varepsilon}{\partial x_j}\right) \quad (7)$$

$$C_{1\varepsilon} = 1.42, C_\mu = 0.0845, C_{2\varepsilon} = 1.68, \Pr_t = 0.85, \sigma_k = 1, \sigma_\varepsilon = 1.3 \quad (8)$$

The available CFD solver ANSYS FLUENT 18.1 has been utilized for simulation according to ref. [81]. Setting up the simulation as an important step is based on [81]. Single-phase fluid with relation similar to [81] was implemented to reduce the computational cost. Selecting Mixture of nanoparticles and H2O is based on [81].

$S_{gen,tot}$ can be derived by sum of $S_{gen,th}$ and $S_{gen,f}$ as expressed by Eq(15). The definitions are as follows:

$$S_{gen,total} = S_{gen,th} + S_{gen,f} \tag{9}$$
$$= \frac{k_{nf}}{T^2}\left[\left(\frac{\partial T}{\partial x}\right)^2 + \left(\frac{\partial T}{\partial y}\right)^2 + \left(\frac{\partial T}{\partial z}\right)^2\right]$$
$$+ \frac{\mu_{nf}}{T}\left\{\begin{array}{l} 2\left[\left(\frac{\partial u_x}{\partial x}\right)^2 + \left(\frac{\partial u_y}{\partial y}\right)^2 + \left(\frac{\partial u_z}{\partial z}\right)^2\right] + \\ \left(\frac{\partial u_x}{\partial y} + \frac{\partial u_y}{\partial x}\right)^2 + \left(\frac{\partial u_x}{\partial z} + \frac{\partial u_z}{\partial x}\right)^2 + \left(\frac{\partial u_y}{\partial z} + \frac{\partial u_z}{\partial y}\right)^2 \end{array}\right\}$$

3. Results and discussion

In current numerical paper, Forced convection of nanofluid for the pipe outfitted via turbulator is investigated. The studied case is heated with uniform heat flux imposed at the wall. Since the behavior of thermal irreversibility is reduced by utilizing nanoparticles, a water-based nanofluid consists of copper oxide as carrier fluid was implemented in the current article.

The outputs reveal that the fluid motion enhances and stronger swirl flow produces, following the turbulator insertion. We repeated the simulation by applying different width tapes in different Reynolds number ranging from 5000–15000. The results of current numerical work have been compared with the output data of [82] based on h(x). As it is evident from Fig 2, close agreement exist between the results.

Figs. 3, 4, 5, 6, 7 and 8, show contours for different values of *b* and *Re*. Following turbulator insertion, entropy generation declines and enhancement of convective flow is observed. As Re number increases, the pressure loss rises and as a result, greater convective flow can be achieved. For cases which include greater flow rate, reducing the inlet velocity resulted in more uniform temperature distribution. $S_{gen,th}$ increases with the increase in ∇T . Improving convective flow leads to increasing Differential pressure. Thus, Δp increases by increasing amounts of *Re* and *b*. On the other hand, since at lower b and Re, turbulence intensity is weaker, Nuselt number reduces following the reduction of b and Re. With decreasing the Nusselt number the parameters *b* and *Re* will be reduced. It can be attributed to lower turbulence at lower *Re and b*.

Turbulent intensity is directly related to width as well as inlet velocity. Thus, utilizing greater input velocity and width increase the turbulent intensity. As a result of increasing b, thermal boundary layer will be more disrupted which resulted in more viscous loss. By increasing the width of turbulator, residence time enhances and it is also observed for Reynolds number. The effect of *Re* is more remarkable compared to *b*, in view of disrupting boundary layer.

The effect of changing Reynolds number and width on $S_{gen,f}$ and $S_{gen,th}$ is shown in Fig. 9. The correlations in association with active factors are proposed in equations 10 and 11 respectively:

$$S_{gen,f} = 0.02 + 0.017\,\mathrm{Re}^* + 5.14\times10^{-3} b + 4.38\times10^{-3} b\,\mathrm{Re}^* + 1.495\times10^{-3} b^2 \tag{10}$$

$$S_{gen,th} = 18.69 - 15.05\,\mathrm{Re}^* - 0.25b + 0.28b\,\mathrm{Re}^* - 0.24b^2 \tag{11}$$

The strength of vortex is augmented with increasing b and this causes larger amounts of Δp. The greater Δp means that the higher $S_{gen,f}$ will be provided. Following an increase in width, temperature gradient declines. As a result, $S_{gen,th}$ decreases. By improving flow rate, more uniform temperature distribution is observed which leads to decrease of $S_{gen,th}$. Since tangential velocity augments with increasing Re, the larger Re causes higher $S_{gen,f}$. The effect of Re on $S_{gen,f}$ is more remarkable comparing with width tape. Besides, in lower pumping power, the impact of *b* on $S_{gen,f}$ is more noticeable. In lower Re, impact of *b* on $S_{gen,f}$ is more noticeable. Also, width tape demonstrates a less influence on $S_{gen,th}$ comparison to Re.

4. Conclusion

The analysis of thermal features of the pipe outfitted by a turbulator has been carried out using computational fluid dynamics. It was observed that using complicated turbulator in addition to nanoparticles as testing fluid is helpful to detect better efficiency. It is also possible to apply this configuration to energy recovery units. Dimensional characteristics of turbulator are investigated and the results can be summarized as follows:

- Following using turbulator, inducing turbulence happens and this impact is more predominant at small Reynolds numbers.
- Concerning greater residence time, Using larger width and inlet velocity leads to turbulence intensity increase.
- Convective flow and turbulent intensity are directly related to width of turbulator.

References

[1] S.U.S. Choi, J. Eastman, Enhancing thermal conductivity of fluids with nanoparticles, ASME-Publications 231 (1995) 99-106.

[2] R. Ellahi, A. Riaz, S. Nadeem, A theoretical study of Prandtl nanofluid in a rectangular duct through peristaltic transport, Applied Nanoscience, Vol. 4, No. 6, pp 753-760 (2014).

[3] NS Bondareva, MA Sheremet, HF Oztop, N Abu-Hamdeh, Entropy generation due to natural convection of a nanofluid in a partially open triangular cavity, Advanced Powder Technology 28 (1), (2017) 244-255

[4] M. Sheikholeslami, Behnoush Rezaeianjouybari, Milad Darzi, Ahmad Shafee, Zhixiong Li, Truong Khang Nguyen, Application of nano-refrigerant for boiling heat transfer

enhancement employing an experimental study, International Journal of Heat and Mass Transfer 141 (2019) 974–980

[5] F Selimefendigil, H Öztop, N Abu-Hamdeh, Natural convection and entropy generation in nanofluid filled entrapped trapezoidal cavities under the influence of magnetic field, Entropy 18 (2), 43 (2016)

[6] M. Sheikholeslami, M. Jafaryar, Jagar A. Ali, Samir Mustafa Hamad, Alireza Divsalar, Ahmad Shafee, Trung Nguyen-Thoi, Zhixiong Li, Simulation of turbulent flow of nanofluid due to existence of new effective turbulator involving entropy generation, Journal of Molecular Liquids 291 (2019) 111283

[7] M. Sheikholeslami, M. Jafaryar, Mohammadali Hedayat, Ahmad Shafee, Zhixiong Li, Truong Khang Nguyen, Mohsen Bakouri, Heat transfer and turbulent simulation of nanomaterial due to compound turbulator including irreversibility analysis, International Journal of Heat and Mass Transfer, 137 (2019) 1290–1300

[8] Seyyed Ali Farshad, M. Sheikholeslami, Nanofluid flow inside a solar collector utilizing twisted tape considering exergy and entropy analysis, Renewable Energy, 141 (2019) 246-258

[9] L Kolsi, HF Oztop, A Alghamdi, N Abu-Hamdeh, MN Borjini, HB Aissia, A computational work on a three dimensional analysis of natural convection and entropy generation in nanofluid filled enclosures with triangular solid insert at the corners, Journal of molecular liquids 218, 260-274

[10] M. Sheikholeslami, Alireza Zareei, M. Jafaryar, Ahmad Shafee, Zhixiong Li, Amor Smida, I. Tlili, Heat transfer simulation during charging of nanoparticle enhanced PCM within a channel, Physica A: Statistical Mechanics and its Applications, 525 (2019) 557–565

[11] M. Sheikholeslami, M. Jafaryar, Ahmad Shafee, Zhixiong Li, Rizwan-ul Haq, Heat transfer of nanoparticles employing innovative turbulator considering entropy generation, International Journal of Heat and Mass Transfer 136 (2019) 1233–1240

[12] M. Sheikholeslami, A. Ghasemi, Solidification heat transfer of nanofluid in existence of thermal radiation by means of FEM, International Journal of Heat and Mass Transfer 123 (2018) 418–431

[13] M. Sheikholeslami, M. Shamlooei, Fe3O4- H2O nanofluid natural convection in presence of thermal radiation, International Journal of Hydrogen Energy, 42(9) (2017) 5708–5718

[14] J. Wu, J. Zhao, J. Lei, B. Liu, Effectiveness of nanofluid on improving the performance of microchannel heat sink, Applied Thermal Engineering 101 (2016) 402-412.

[15] H.E. Ahmed, M.I. Ahmed, I.M.F. Seder, B.H. Salman, Experimental investigation for sequential triangular double-layered microchannel heat sink with nanofluids, International Communications in Heat and Mass Transfer 77 (2016) 104-115.

[16] G.-S. Wang, B. Song, Z.-H. Liu, Operation characteristics of cylindrical miniature grooved heat pipe using aqueous CuO nanofluids, Experimental Thermal and Fluid Science 34(8) (2010) 1415-1421.

[17] W. Gao, W. F. Wang, M. R. Farahani, Topological indices study of molecular structure in anticancer drugs, Journal of Chemistry, Volume 2016, Article ID 3216327, 8 pages, http://dx.doi.org/10.1155/2016/3216327.

[18] M. Sheikholeslami, M. Jafaryar, Ahmad Shafee, Zhixiong Li, Hydrothermal and second law behavior for charging of NEPCM in a two dimensional thermal storage unit, Chinese Journal of Physics, 58 (2019) 244-252

[19] W. Gao, W. F. Wang, The vertex version of weighted wiener number for bicyclic molecular structures, Computational and Mathematical Methods in Medicine, Volume 2015, Article ID 418106, 10 pages, http://dx.doi.org/10.1155/2015/418106.

[20] Mohsen Sheikholeslami, Ahmad Arabkoohsar, Ilyas Khan, Ahmad Shafee, Zhixiong Li, Impact of Lorentz forces on Fe3O4-water ferrofluid entropy and exergy treatment within a permeable semi annulus, Journal of Cleaner Production, 221 (2019) 885-898

[21] W. Gao, W. F. Wang, Second atom-bond connectivity index of special chemical molecular structures, Journal of Chemistry, Volume 2014, Article ID 906254, 8 pages, http://dx.doi.org/10.1155/2014/906254.

[22] M. Sheikholeslami, M. Jafaryar, Ahmad Shafee, Zhixiong Li, Simulation of nanoparticles application for expediting melting of PCM inside a finned enclosure, Physica A: Statistical Mechanics and its Applications 523 (2019) 544–556

[23] W. Gao, L. L. Zhu, K. Y. Wang, Ontology sparse vector learning algorithm for ontology similarity measuring and ontology mapping via ADAL technology, International Journal of Bifurcation and Chaos, 2015, 25(14) , 1540034 (12 pages), DOI: 10.1142/S0218127415400349.

[24] M. Sheikholeslami, S. A. M. Mehryan, Ahmad Shafee, Mikhail A. Sheremet, Variable magnetic forces impact on Magnetizable hybrid nanofluid heat transfer through a circular cavity, Journal of Molecular Liquids, 277 (2019) 388-396

[25] W. Gao, L. L. Zhu, Gradient learning algorithms for ontology computing, Computational Intelligence and Neuroscience, Volume 2014, Article ID 438291, 12 pages, http://dx.doi.org/10.1155/2014/438291.

[26] M. Sheikholeslami, Omid Mahian, Enhancement of PCM solidification using inorganic nanoparticles and an external magnetic field with application in energy storage systems, Journal of Cleaner Production 215 (2019) 963-977

[27] W. Gao, W. F. Wang, M. K. Jamil, M. R. Farahani, Electron energy studying of molecular structures via forgotten topological index computation, Journal of Chemistry, Volume 2016, Article ID 1053183, 7 pages, http://dx.doi.org/10.1155/2016/1053183.

[28] W. Gao, M. R. Farahani, L. Shi, The forgotten topological index of some drug structures, Acta Medica Mediterranea, 2016, 32: 579-585.

[29] M. Sheikholeslami, Rizwan-ul Haq, Ahmad Shafee, Zhixiong Li, Yassir G. Elaraki, I. Tlili, Heat transfer simulation of heat storage unit with nanoparticles and fins through a heat exchanger, International Journal of Heat and Mass Transfer 135 (2019) 470–478

[30] W. Gao, M. K. Siddiqui, M. Imran, M. K. Jamil, M. R. Farahani, Forgotten topological index of chemical structure in drugs, Saudi Pharmaceutical Journal, 2016, 24(3): 258-264.

[31] M. Sheikholeslami, Application of Darcy law for nanofluid flow in a porous cavity under the impact of Lorentz forces, Journal of Molecular Liquids 266 (2018) 495–503

[32] M. Sheikholeslami, Rizwan-ul Haq, Ahmad Shafee, Zhixiong Li, Heat transfer behavior of Nanoparticle enhanced PCM solidification through an enclosure with V shaped fins, International Journal of Heat and Mass Transfer 130 (2019) 1322–1342

[33] A.M. Abed, M.A. Alghoul, K. Sopian, H.A. Mohammed, H.s. Majdi, A.N. Al-Shamani, Design characteristics of corrugated trapezoidal plate heat exchangers using nanofluids, Chemical Engineering and Processing: Process Intensification 87 (2015) 88-103.

[34] P.V. Durga Prasad, A.V.S.S.K.S. Gupta, M. Sreeramulu, L.S. Sundar, M.K. Singh, A.C.M. Sousa, Experimental study of heat transfer and friction factor of Al2O3 nanofluid in

U-tube heat exchanger with helical tape inserts, Experimental Thermal and Fluid Science 62 (2015) 141-150.

[35] W. Zhang, W. Li, A. Nakayama, An analytical consideration of steady-state forced convection within a nanofluid-saturated metal foam, Journal of Fluid Mechanics 769 (2015) 590-620.

[36] Y. Qin, Y. He, B. Wu, S. Ma, X. Zhang, Regulating top albedo and bottom emissivity of concrete roof tiles for reducing building heat gains, Energy and Buildings 156(Supplement C) (2017) 218-224

[37] M. Sheikholeslami, New computational approach for exergy and entropy analysis of nanofluid under the impact of Lorentz force through a porous media, Computer Methods in Applied Mechanics and Engineering 344 (2019) 319–333

[38] Y. Qin, Pavement surface maximum temperature increases linearly with solar absorption and reciprocal thermal inertial, International Journal of Heat and Mass Transfer, 97 (2016) 391-399

[39] M. Sheikholeslami, Numerical approach for MHD Al2O3-water nanofluid transportation inside a permeable medium using innovative computer method, Computer Methods in Applied Mechanics and Engineering 344 (2019) 306–318

[40] Zehui Shao, Ehsan Gholamalizadeh, Albert Boghosian, Behnam Askarian, Zhenling Liu, The chiller's electricity consumption simulation by considering the demand response program in power system, Applied Thermal Engineering. 149 (2019) ,1114-1124.

[41] M. Sheikholeslami, M. Barzegar Gerdroodbary, R. Moradi, Ahmad Shafee, Zhixiong Li, Application of Neural Network for estimation of heat transfer treatment of Al2O3- H2O

nanofluid through a channel, Computer Methods in Applied Mechanics and Engineering, 344 (2019) 1‑12

[42] Y. Qin, J. Liang, K. Tan, F. Li. A side by side comparison of the cooling effect of building blocks with retro-reflective and diffuse-reflective walls, Solar Energy, 133 (2016) 172–179

[43] M. Sheikholeslami, Magnetic source impact on nanofluid heat transfer using CVFEM, Neural Computing and Applications, Volume 30, Issue 4, (2018), pp 1055–1064

[44] Y. Qin, J. Liang, H. Yang, Z. Deng, Gas permeability of pervious concrete and its implications on the application of pervious pavements, Measurement, 78 (2016) 104-110

[45] Shi, X., Lu, W., Wang, Z., Pan, L., Cui, G., Xu, J., & LaBean, T. H. (2014), Programmable DNA tile self-assembly using a hierarchical sub-tile strategy, Nanotechnology, 25(7), 075602.

[46] M. Sheikholeslami, Application of Darcy law for nanofluid flow in a porous cavity under the impact of Lorentz forces, Journal of Molecular Liquids 266 (2018) 495‑503

[47] Y. Qin, J.E. Hiller, Understanding pavement-surface energy balance and its implications on cool pavement development, Energy and Buildings, 85 (2014) 389-399.

[48] M. Sheikholeslami, M. Jafaryar, S. Saleem, Zhixiong Li, Ahmad Shafee, Yu Jiang, Nanofluid heat transfer augmentation and exergy loss inside a pipe equipped with innovative turbulators, International Journal of Heat and Mass Transfer 126 (2018) 156–163

[49] Y. Qin, M. Zhang, G. Mei, A new simplified method for measuring the permeability characteristics of highly porous media, Journal of Hydrology 562 (2018) 725-732

[50] Zehui Shao, Karzan Wakil, Muhammet Usak, Mohammad Amin Heidari, Bo Wang, Rolando Simoes: Kriging Empirical Mode Decomposition via support vector machine learning technique for autonomous operation diagnosing of CHP in microgrid, Applied Thermal Engineering. 145 (2018) 58-70.

[51] M. Sheikholeslami, A. Ghasemi, Zhixiong Li, Ahmad Shafee, S. Saleem, Influence of CuO nanoparticles on heat transfer behavior of PCM in solidification process considering radiative source term, International Journal of Heat and Mass Transfer 126 (2018) 1252–1264

[52] Y. Qin, Urban canyon albedo and its implication on the use of reflective cool pavements, Energy and Buildings, 96 (2015) 86-94

[53] M. Sheikholeslami, A. Zeeshan, Analysis of flow and heat transfer in water based nanofluid due to magnetic field in a porous enclosure with constant heat flux using CVFEM, Computer Methods in Applied Mechanics and Engineering, 320 (2017) 68–81

[54] W. Gao, W. F. Wang, The eccentric connectivity polynomial of two classes of nanotubes, Chaos, Solitons and Fractals, 2016, 89: 290–294.

[55] M. Sheikholeslami, K. Vajravelu, Nanofluid flow and heat transfer in a cavity with variable magnetic field, Applied Mathematics and Computation, 298 (2017) 272–282

[56] Yinghong Qin, Jacob E. Hiller and Demiao Meng. Linearity between pavement thermophysical properties and surface temperatures. Journal of Materials in Civil Engineering, 2019. https://doi.org/10.1061/(ASCE)MT.1943-5533.0002890

[57] M. Sheikholeslami, Milad Darzi, MK Sadoughi, Heat transfer improvement and Pressure Drop during condensation of refrigerant-based Nanofluid; An Experimental Procedure, International Journal of Heat and Mass Transfer 122 (2018) 643–650.

[58] Qin Y, Luo J, Chen Z, Mei G, Yan L-E, Measuring the albedo of limited-extent targets without the aid of known-albedo masks, Solar Energy 171(2018) 971-976

[59] Y. Qin, A review on the development of cool pavements to mitigate urban heat island effect, Renewable and Sustainable Energy Reviews, 52 (2015) 445-459

[60] M. Sheikholeslami, Numerical modeling of Nano enhanced PCM solidification in an enclosure with metallic fin, Journal of Molecular Liquids 259 (2018) 424–438

[61] Qin Y, He Y, Hiller JE, Mei G, A new water-retaining paver block for reducing runoff and cooling pavement. Journal of Cleaner Production 199 (2018) 948-956

[62] M. Sheikholeslami, Solidification of NEPCM under the effect of magnetic field in a porous thermal energy storage enclosure using CuO nanoparticles, Journal of Molecular Liquids 263 (2018) 303–315

[63] Qin, Y., Zhao, Y., Chen, X., Wang, L., Li, F., Bao, T., Moist curing increases the solar reflectance of concrete. Construction and Building Materials 215(2019) 114-118.

[64] Mohsen Sheikholeslami, Numerical simulation for solidification in a LHTESS by means of Nano-enhanced PCM, Journal of the Taiwan Institute of Chemical Engineers 86 (2018) 25–41

[65] Y. Qin, M. Zhang, J.E. Hiller, Theoretical and experimental studies on the daily accumulative heat gain from cool roofs, Energy, 129 (2017) 138-147

[66] M. Sheikholeslami, Influence of magnetic field on Al2O3-H2O nanofluid forced convection heat transfer in a porous lid driven cavity with hot sphere obstacle by means of LBM, Journal of Molecular Liquids 263 (2018) 472–488

[76] Mohsen Sheikholeslami, Houman B. Rokni, Melting heat transfer influence on nanofluid flow inside a cavity in existence of magnetic field, International Journal of Heat and Mass Transfer 114 (2017) 517–526

[68] Y. Qin, H. He, A new simplified method for measuring the albedo of limited extent targets, Solar Energy 157(Supplement C) (2017) 1047-1055

[69] M. Sheikholeslami, Finite element method for PCM solidification in existence of CuO nanoparticles, Journal of Molecular Liquids 265 (2018) 347–355

[70] M. Sheikholeslami, Houman B. Rokni, Magnetic nanofluid flow and convective heat transfer in a porous cavity considering Brownian motion effects, Physics of Fluids, Volume 30, Issue 1, (2018), 10.1063/1.5012517, https://doi.org/10.1063/1.5012517

[71] W. Gao, L. Yan, L. Shi, Generalized Zagreb index of polyomino chains and nanotubes, Optoelectronics and Advanced Materials – Rapid Communications, 2017, 11(1-2): 119-124.

[72] Mohsen Sheikholeslami, Magnetic field influence on CuO -H2O nanofluid convective flow in a permeable cavity considering various shapes for nanoparticles, International Journal of Hydrogen Energy, 42 (2017) 19611-19621

[73] S. Nadeem, Arshad Riaz, R. Ellahi, N. S. Akbar, Mathematical model for the peristaltic flow of Jeffrey fluid with nanoparticles phenomenon through a rectangular duct, Applied Nanoscience, Vol 4, 613-624 (2014).

[74] S. Nadeem, Arshad Riaz, R. Ellahi, N. S. Akbar, Effects of heat and mass transfer on peristaltic flow of a nanofluid between eccentric cylinders, Applied Nanoscience, Vol 4, 393-404 (2014).

[75] S. Nadeem, Arshad Riaz, R. Ellahi, N. S. Akbar, Mathematical model for the peristaltic flow of nanofluid through eccentric tubes comprising porous medium" Applied Nanoscience,

Vol. 4, 733-743 (2014).

[76] A el malik Bouchoucha, R Bessaïh, HF Oztop, K Al-Salem, F Bayrak, Natural convection and entropy generation in a nanofluid filled cavity with thick bottom wall: Effects of non-isothermal heating, International Journal of Mechanical Sciences 126, (2017) 95-105

[77] E Abu-Nada, HF Oztop, Effects of inclination angle on natural convection in enclosures filled with Cu-water nanofluid, International Journal of Heat and Fluid Flow 30 (4), 669-678, 2009

[78] L. Asmaie, M. Haghshenasfard, A. Mehrabani-Zeinabad, M. Nasr Esfahany, Thermal performance analysis of nanofluids in a thermosyphon heat pipe using CFD modeling, Heat and Mass Transfer 49(5) (2013) 667-678.

[79] Y. Xuan, H. Duan, Q. Li, Enhancement of solar energy absorption using a plasmonic nanofluid based on TiO2/Ag composite nanoparticles, RSC Advances 4(31) (2014) 16206-16213.

[80] Seyyed Ali Farshad, M. Sheikholeslami, Nanofluid flow inside a solar collector utilizing twisted tape considering exergy and entropy analysis, Renewable Energy, 141 (2019) 246-258

[81] M. Sheikholeslami, M. Jafaryar, Zhixiong Li, Nanofluid turbulent convective flow in a circular duct with helical turbulators considering CuO nanoparticles, International Journal of Heat and Mass Transfer 124 (2018) 980–989

[82] D. Kim, Y. Kwon, Y. Cho, C. Li, S. Cheong, Y. Hwang, J. Lee, D. Hong, S. Moona, Convective heat transfer characteristics of nanofluids under laminar and turbulent flow conditions, Current Applied Physics 9 (2009) 119–123.

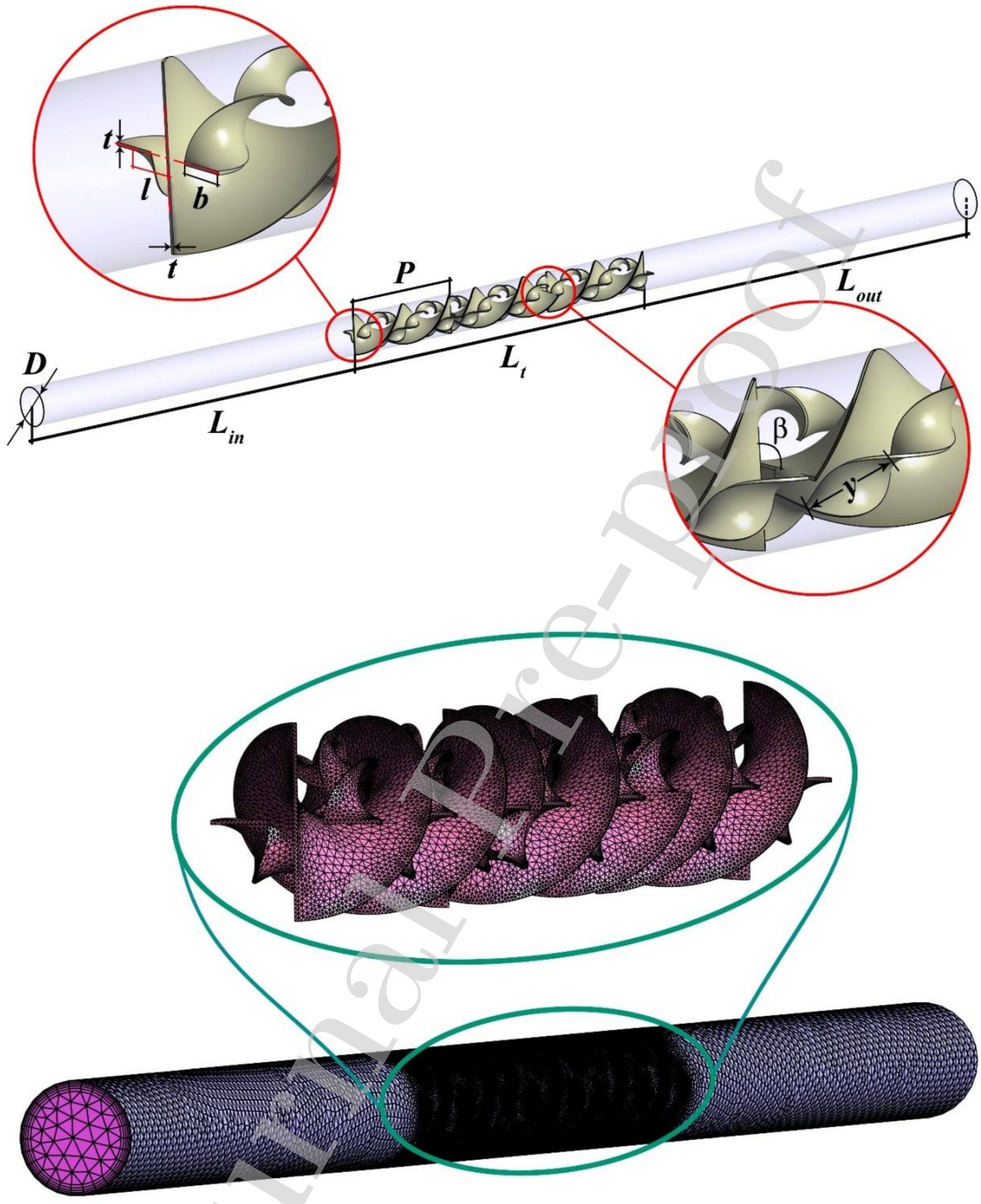

Fig 1. Present pipe and sample mesh.

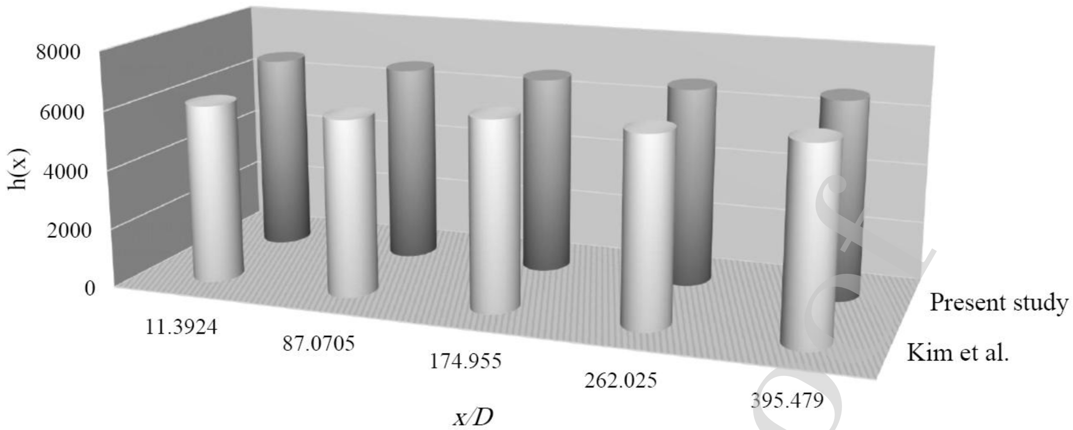

Fig. 2. Comparison of the outputs obtained from [77]

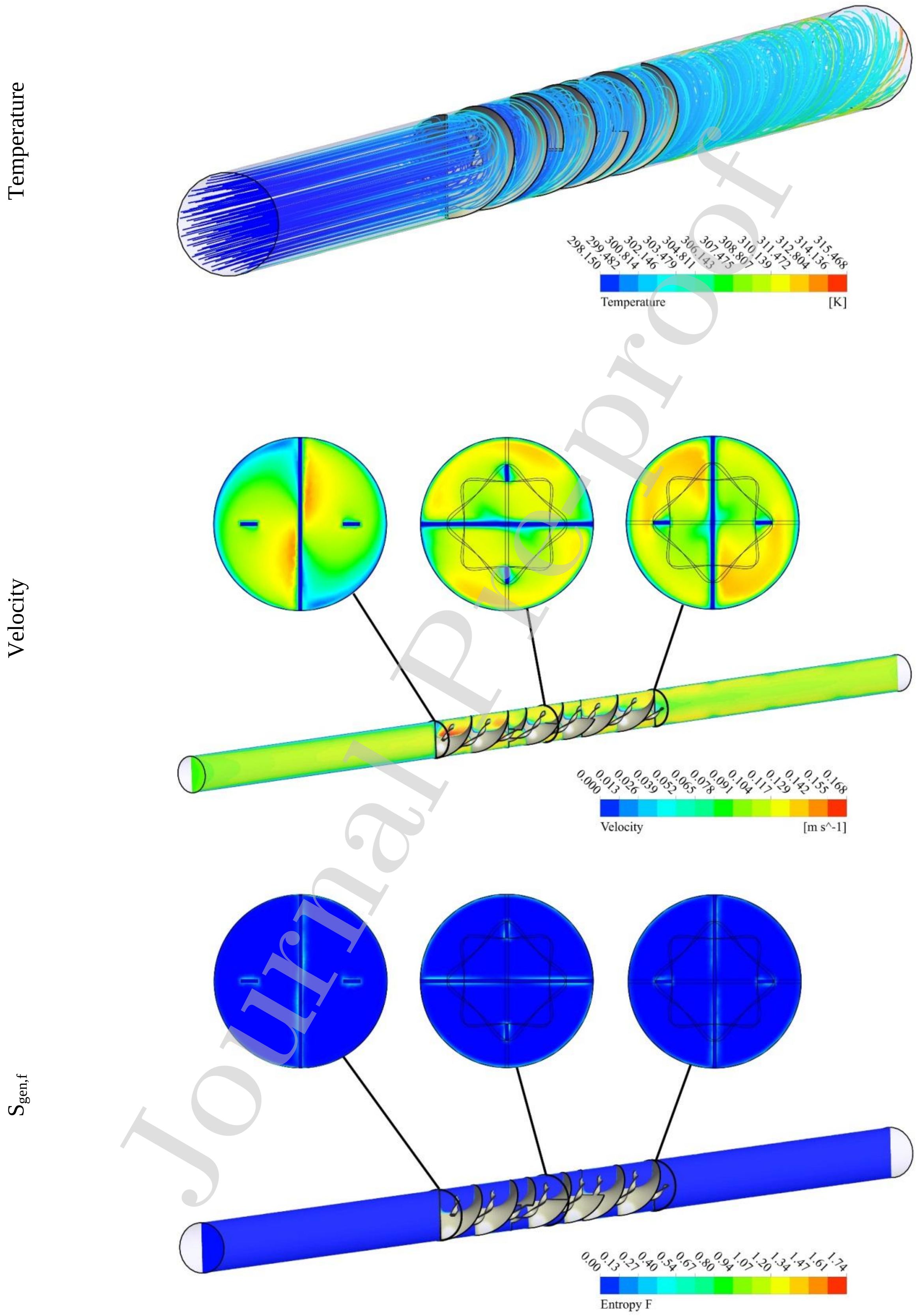
Temperature
298.150 299.482 300.814 302.146 303.479 304.811 306.143 307.475 308.807 310.139 311.472 312.804 314.136 315.468
Temperature
[K]
Velocity
0.000 0.013 0.026 0.039 0.052 0.065 0.078 0.091 0.104 0.117 0.129 0.142 0.155 0.168
Velocity
[m s^-1]
$S_{gen,f}$
0.00 0.13 0.27 0.40 0.54 0.67 0.80 0.94 1.07 1.20 1.34 1.47 1.61 1.74
Entropy F

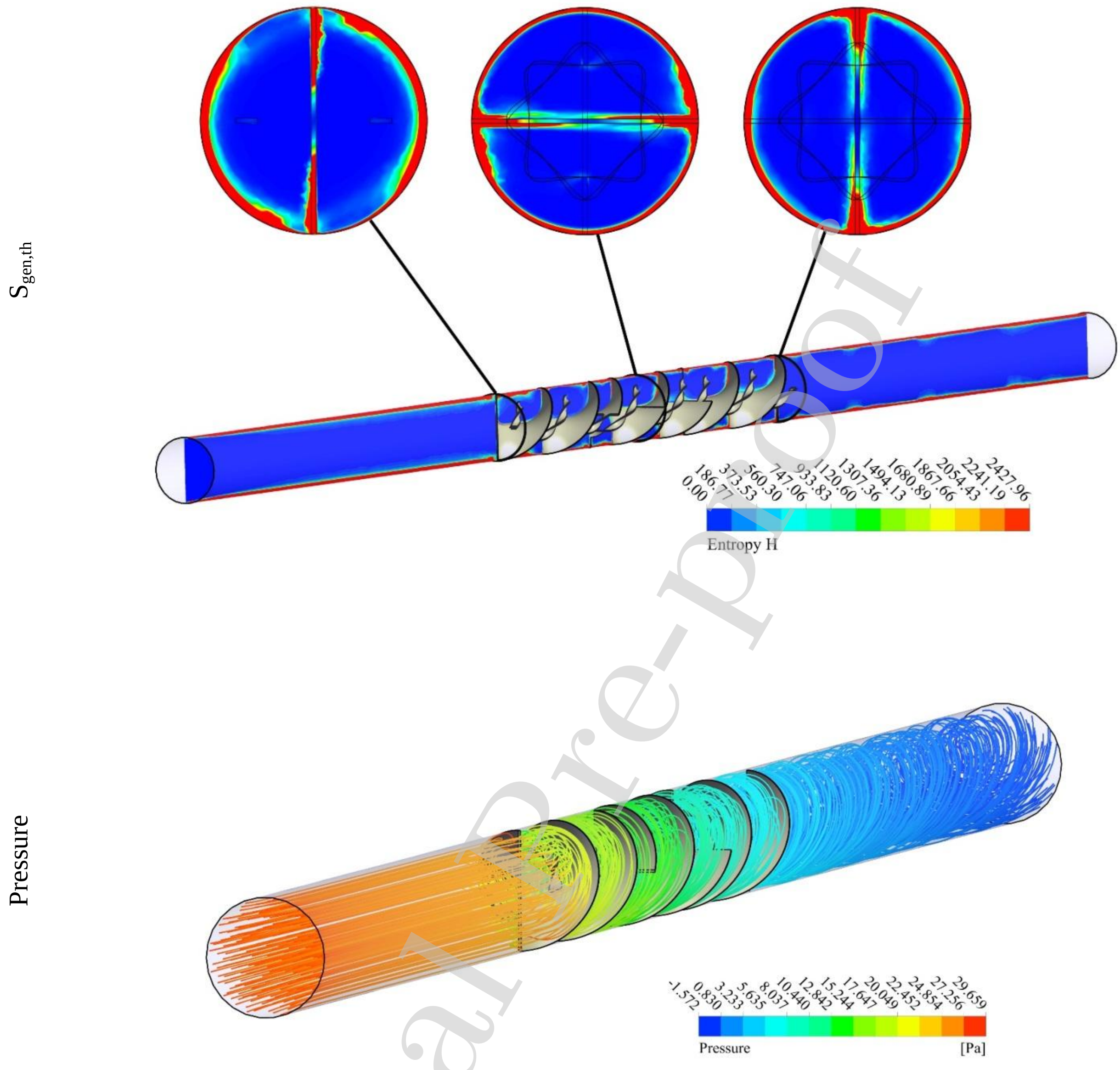

Fig. 3. Velocity, T, P, S_{gen} contours at Re=5000, b=5mm

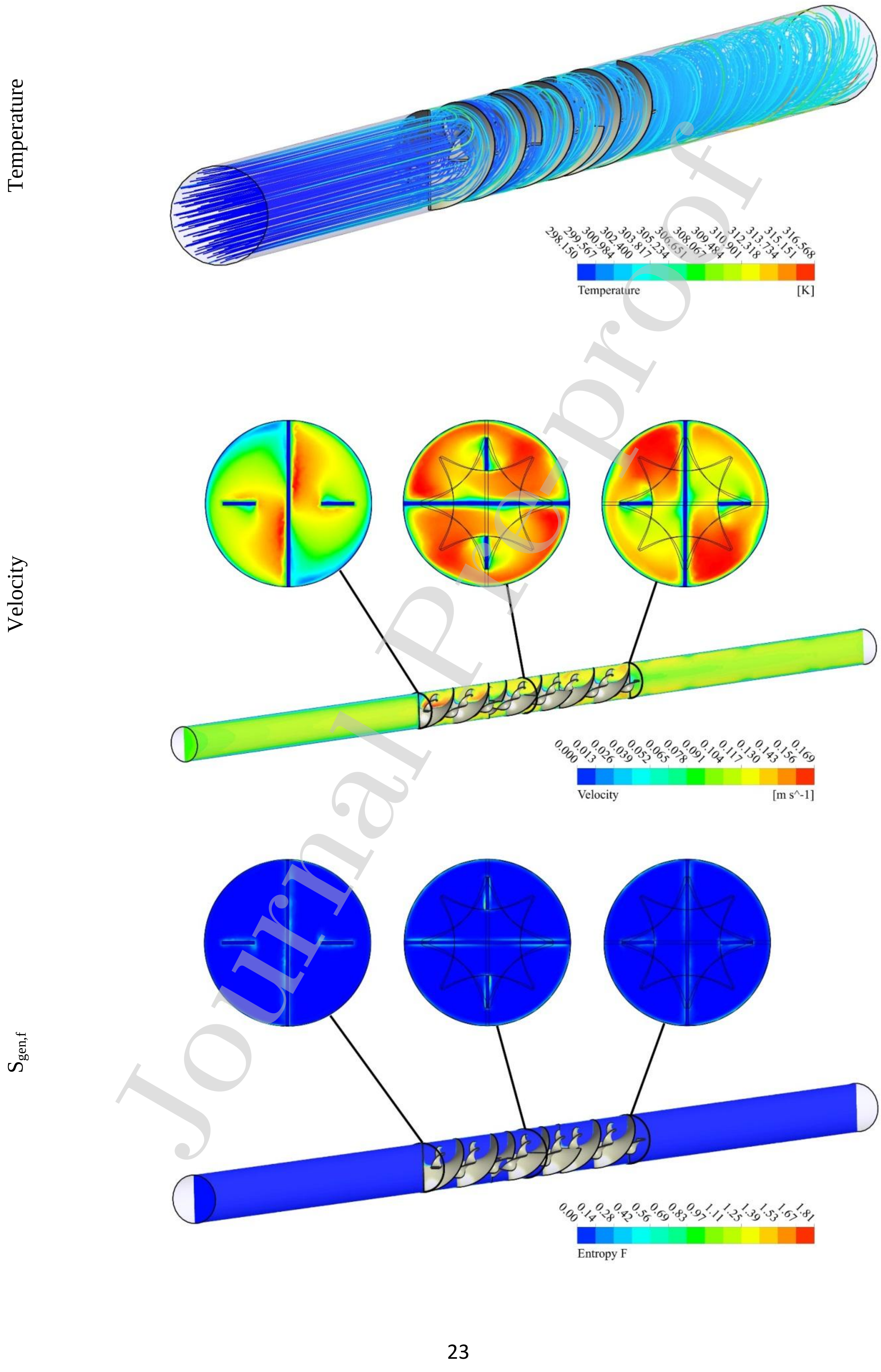

Temperature
298.150
299.567
300.984
302.400
303.817
305.234
306.651
308.067
309.484
310.901
312.318
313.734
315.151
316.568
Temperature
[K]
Velocity
0.000
0.013
0.026
0.039
0.052
0.065
0.078
0.091
0.104
0.117
0.130
0.143
0.156
0.169
Velocity
[m s^-1]
$S_{gen,f}$
0.00
0.14
0.28
0.42
0.56
0.69
0.83
0.97
1.11
1.25
1.39
1.53
1.67
1.81
Entropy F

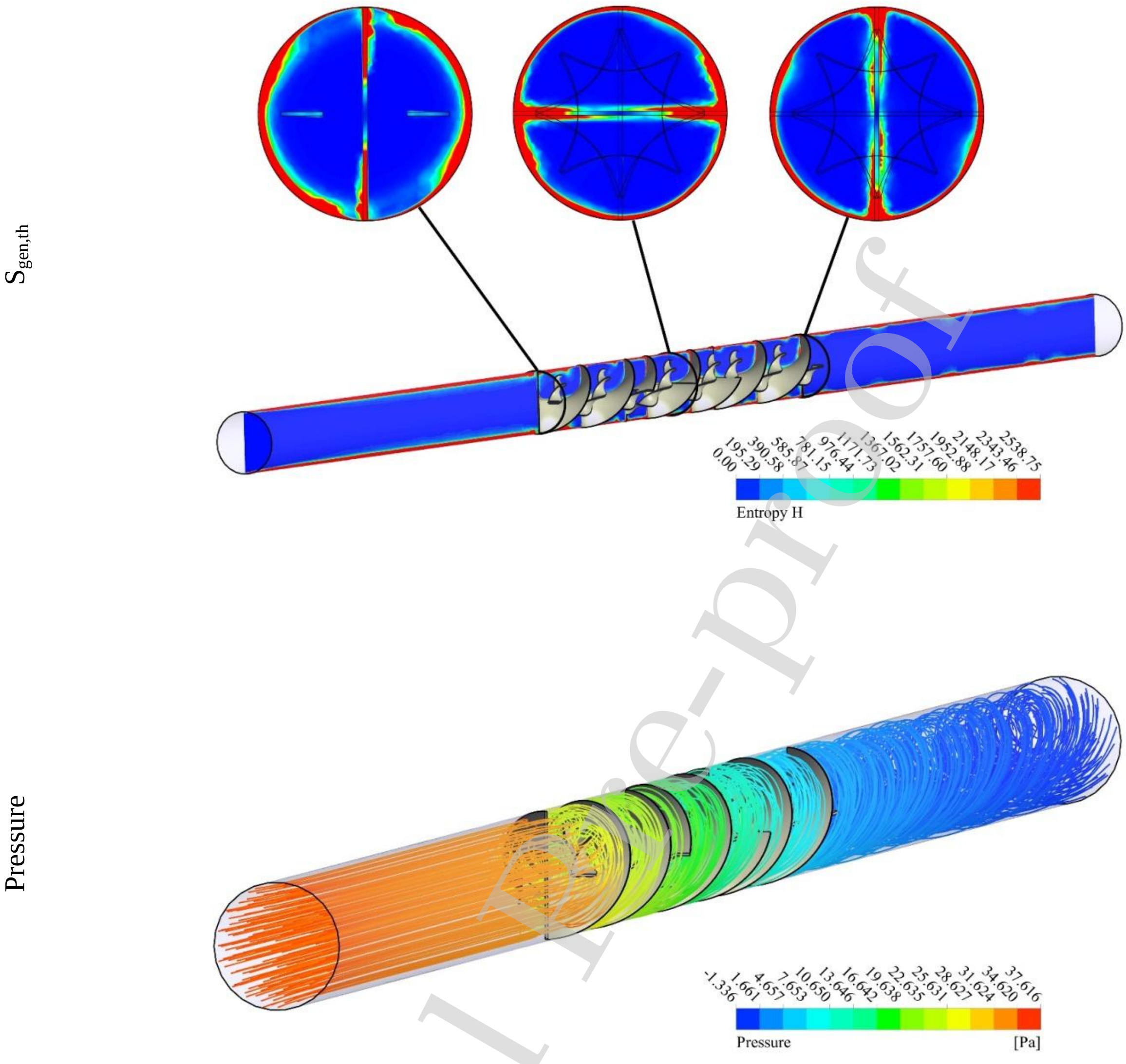

Fig. 4. Velocity, T, P, S_{gen} contours at Re=5000, b=10mm

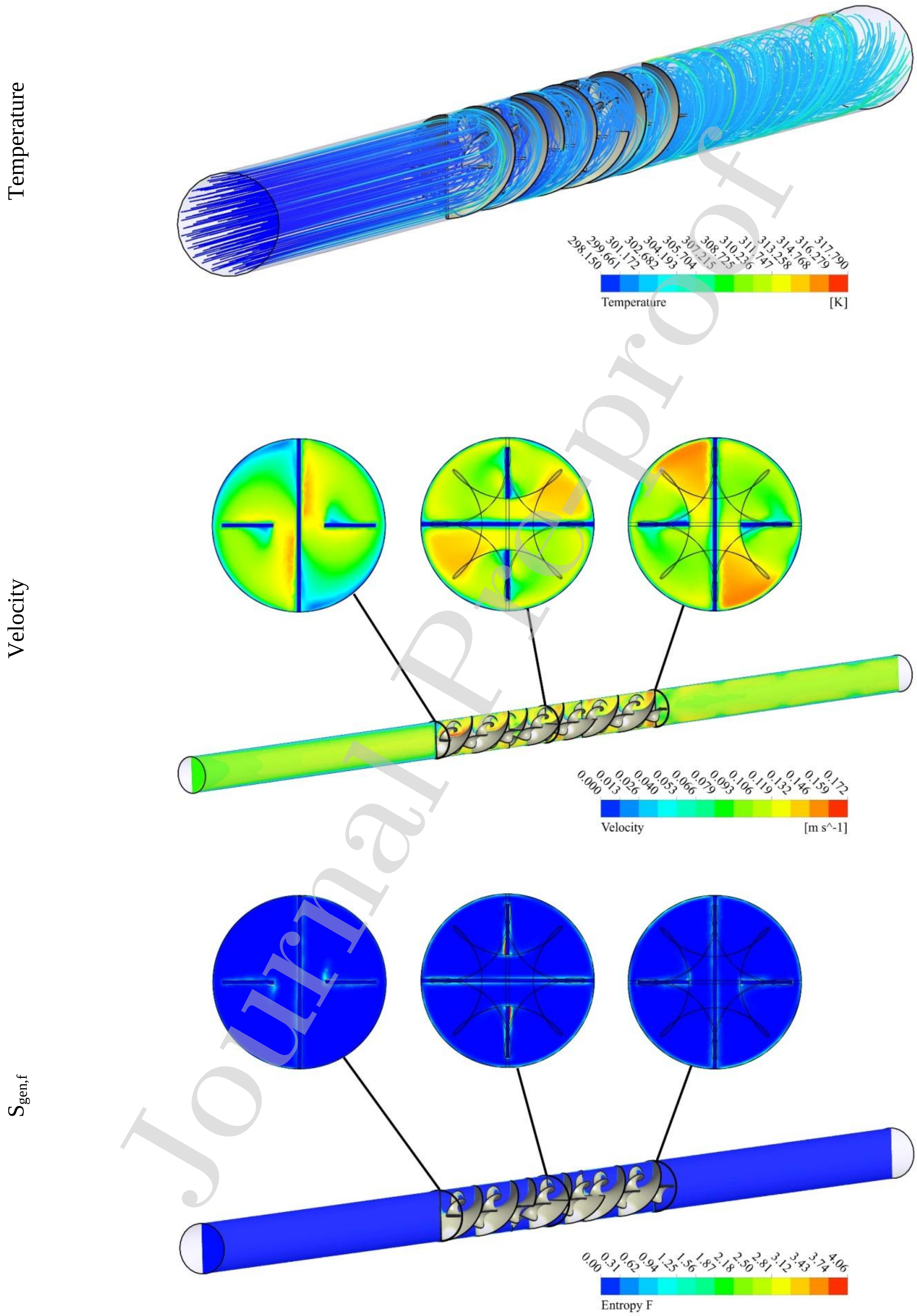

Temperature
298.150 299.661 301.172 302.682 304.193 305.704 307.215 308.725 310.236 311.747 313.258 314.768 316.279 317.790
Temperature [K]
Velocity
0.000 0.013 0.026 0.040 0.053 0.066 0.079 0.093 0.106 0.119 0.132 0.146 0.159 0.172
Velocity [m s^-1]
$S_{gen,f}$
0.00 0.31 0.62 0.94 1.25 1.56 1.87 2.18 2.50 2.81 3.12 3.43 3.74 4.06
Entropy F

$S_{gen,th}$

Pressure

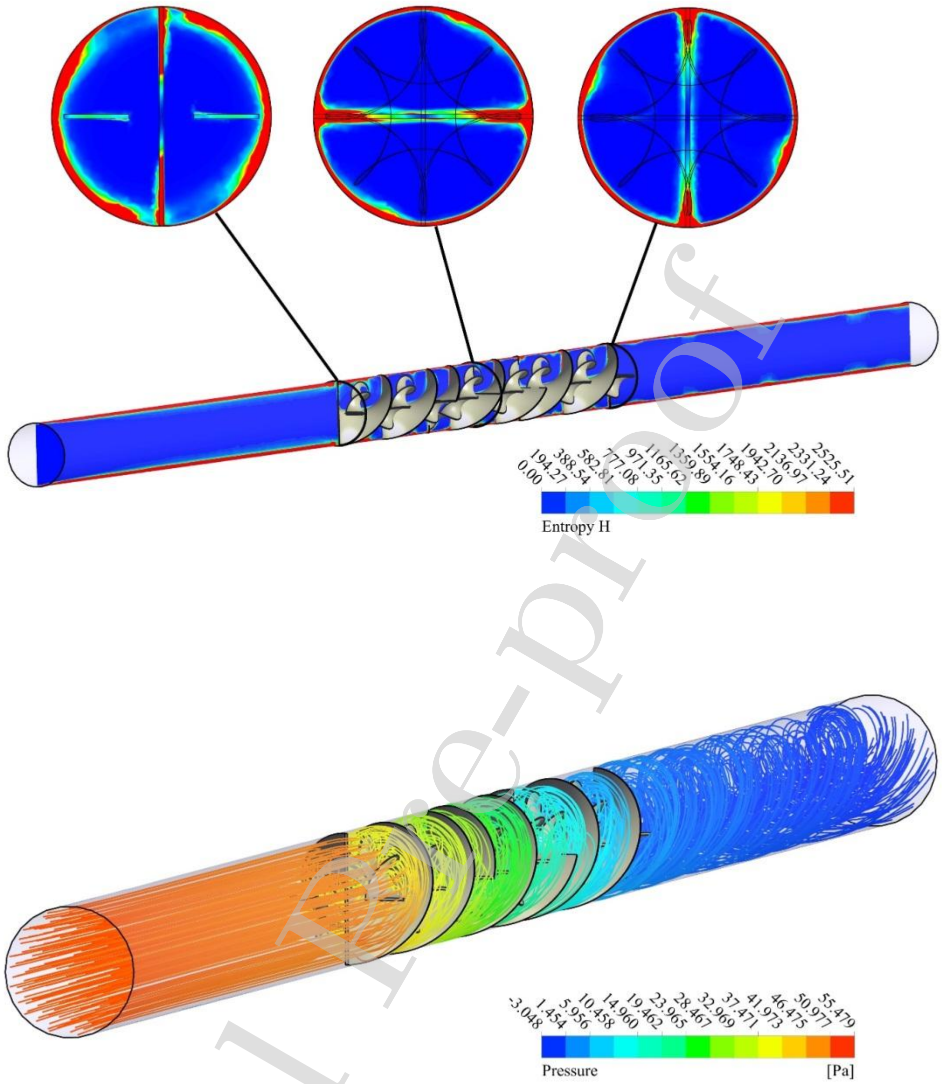

Fig. 5. Velocity, T, P, S_{gen} contours at Re=5000, b=15mm

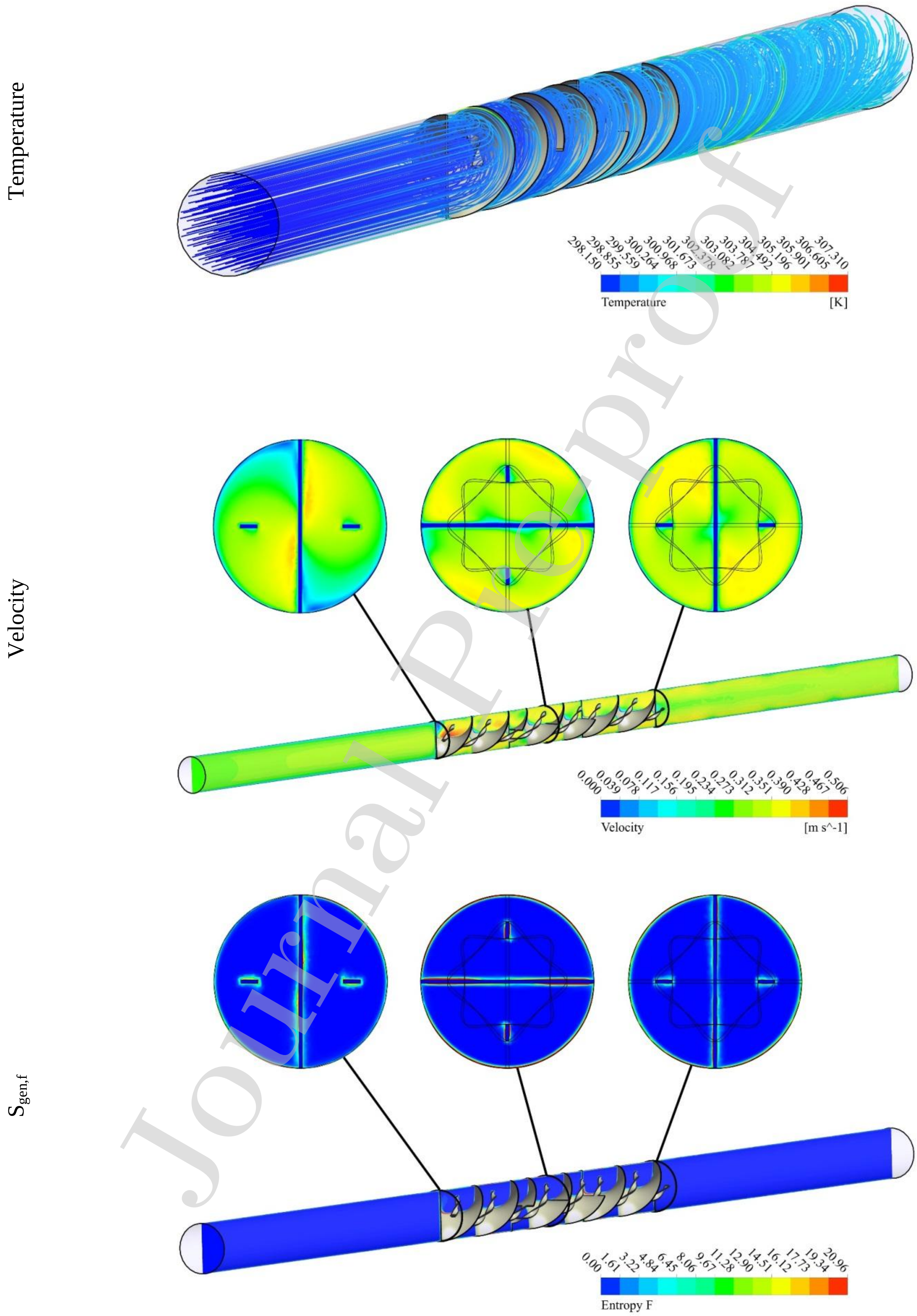

Temperature
298.150
298.855
299.559
300.264
300.968
301.673
302.378
303.082
303.787
304.492
305.196
305.901
306.605
307.310
Temperature
[K]
Velocity
0.000
0.039
0.078
0.117
0.156
0.195
0.234
0.273
0.312
0.351
0.390
0.428
0.467
0.506
Velocity
[m s^-1]
$S_{gen,f}$
0.00
1.61
3.22
4.84
6.45
8.06
9.67
11.28
12.90
14.51
16.12
17.73
19.34
20.96
Entropy F

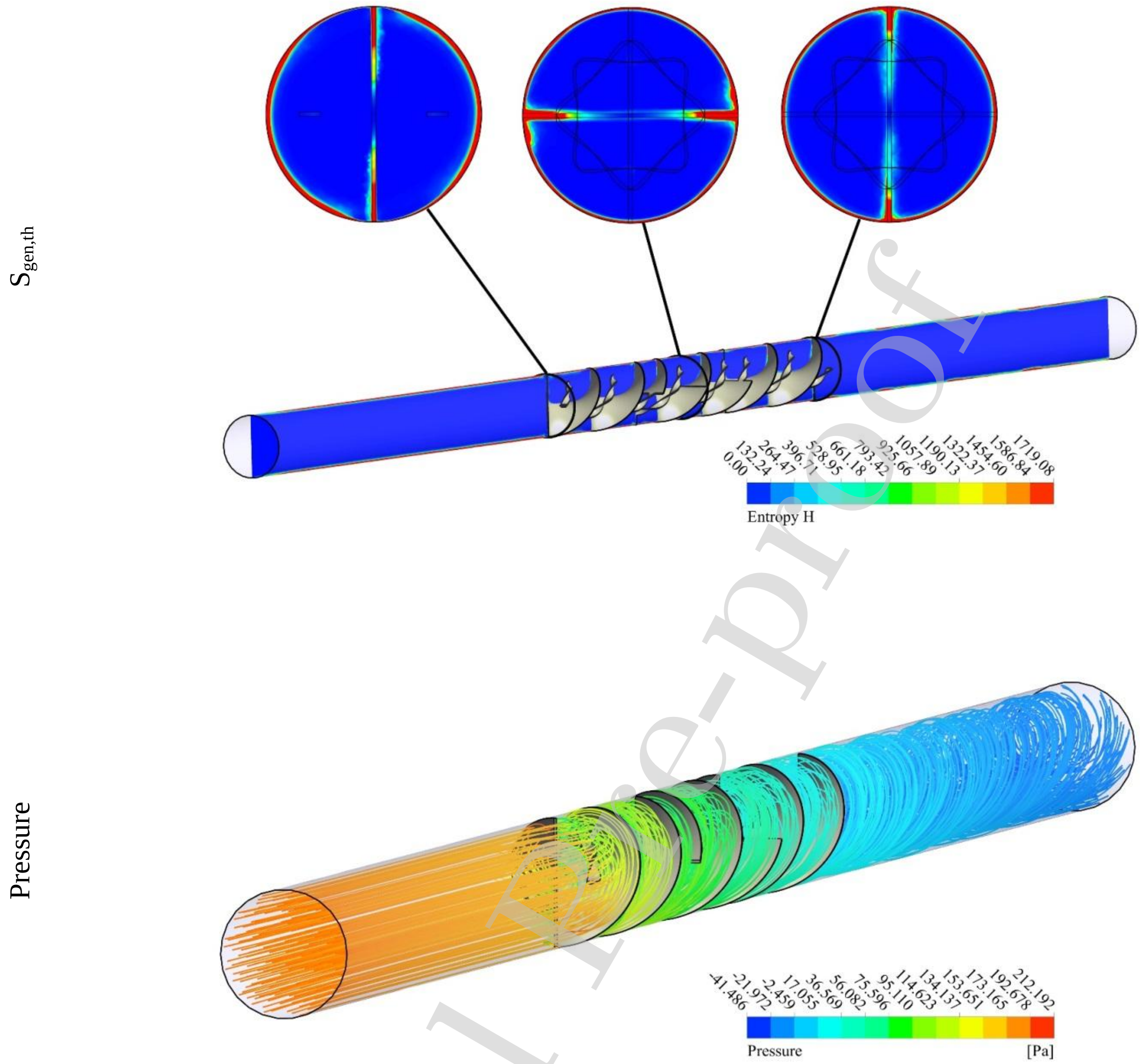

Fig. 6. Velocity, T, P, S_{gen} contours at Re=15000, b=5mm

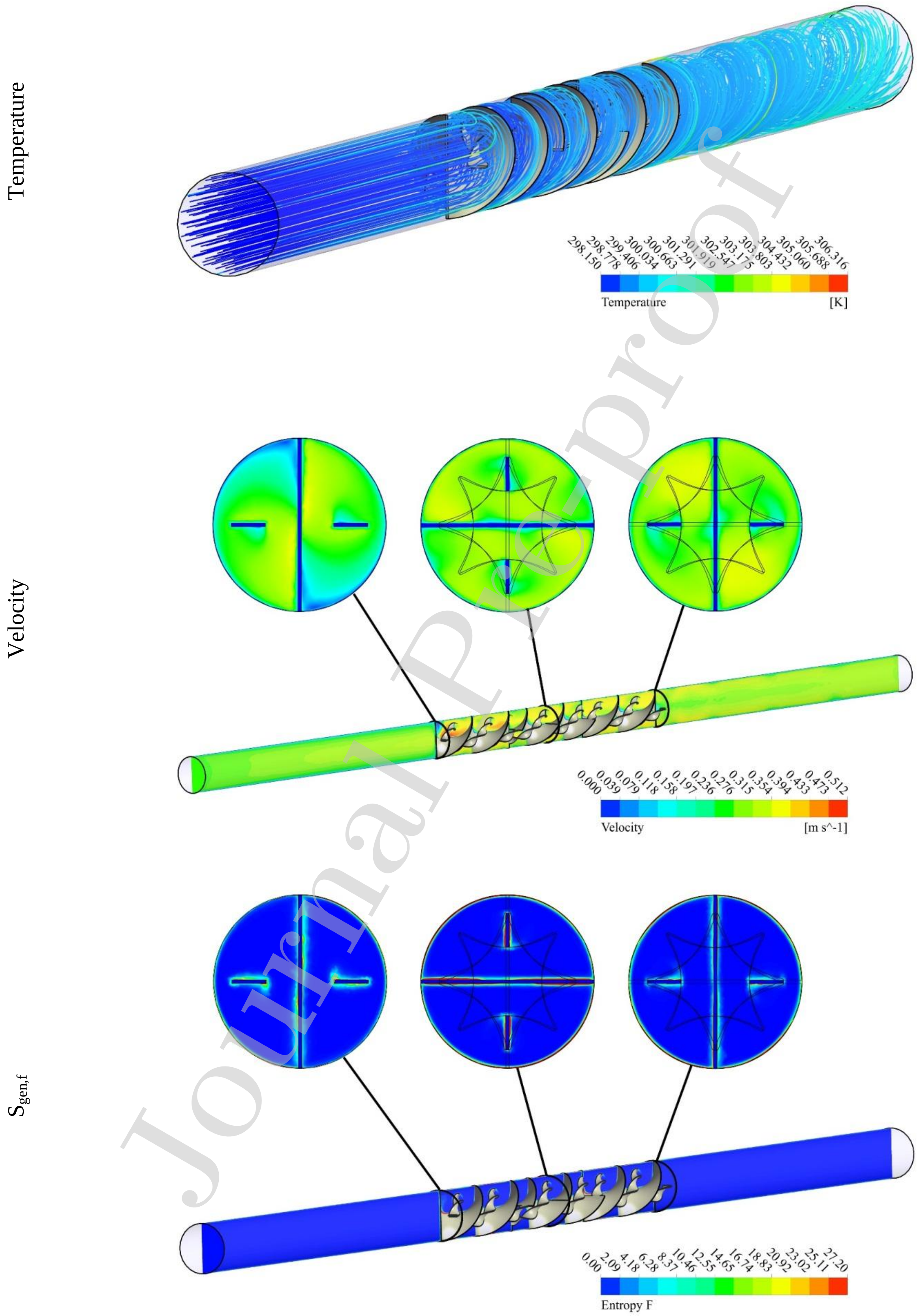
Temperature
298.150
298.778
299.406
300.034
300.663
301.291
301.919
302.547
303.175
303.803
304.432
305.060
305.688
306.316
Temperature
[K]
Velocity
0.000
0.039
0.079
0.118
0.158
0.197
0.236
0.276
0.315
0.354
0.394
0.433
0.473
0.512
Velocity
[m s^-1]
$S_{gen,f}$
0.00
2.09
4.18
6.28
8.37
10.46
12.55
14.65
16.74
18.83
20.92
23.02
25.11
27.20
Entropy F

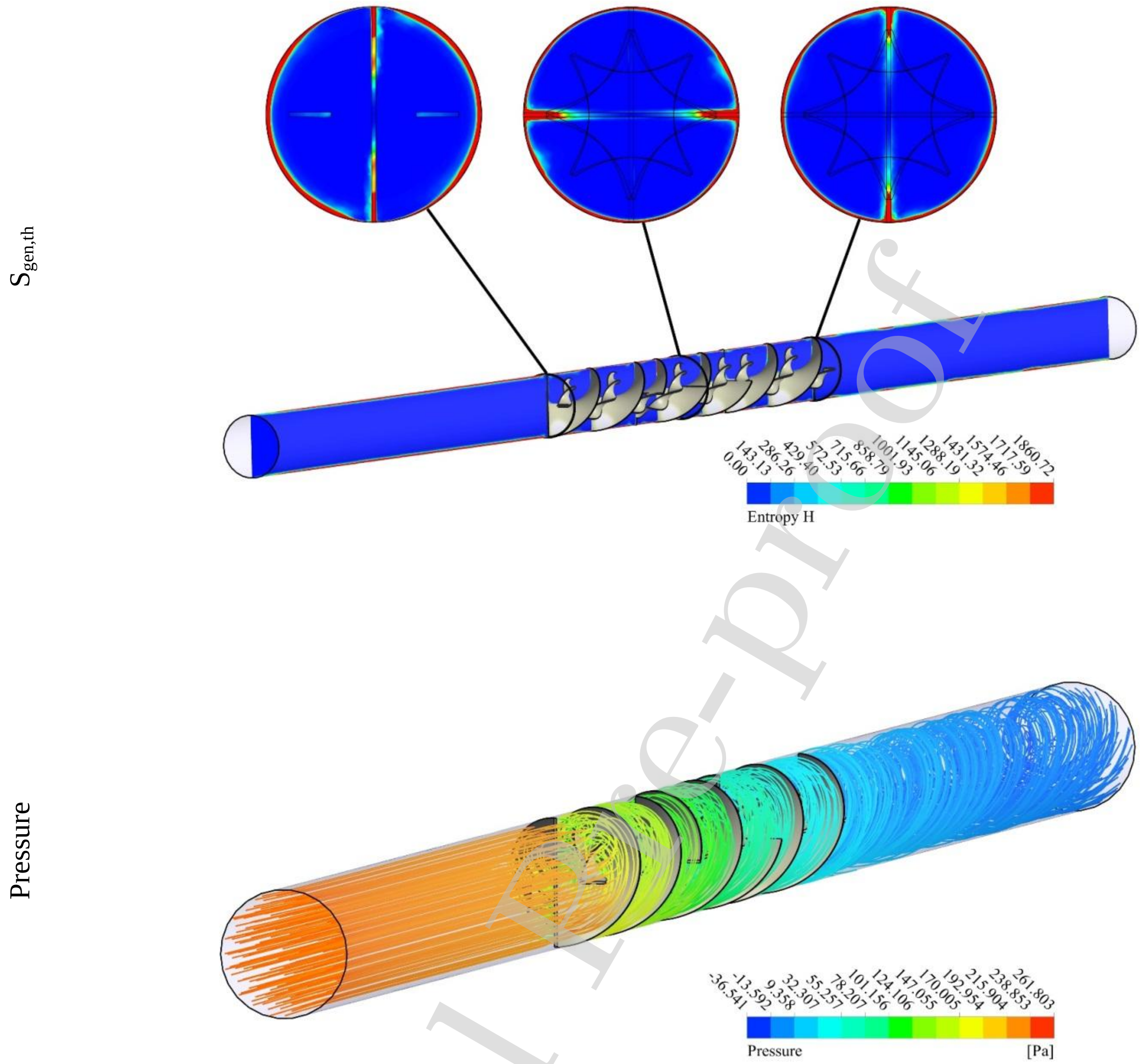

Fig. 7. Velocity, T, P, S_{gen} contours at Re=15000, b=10mm

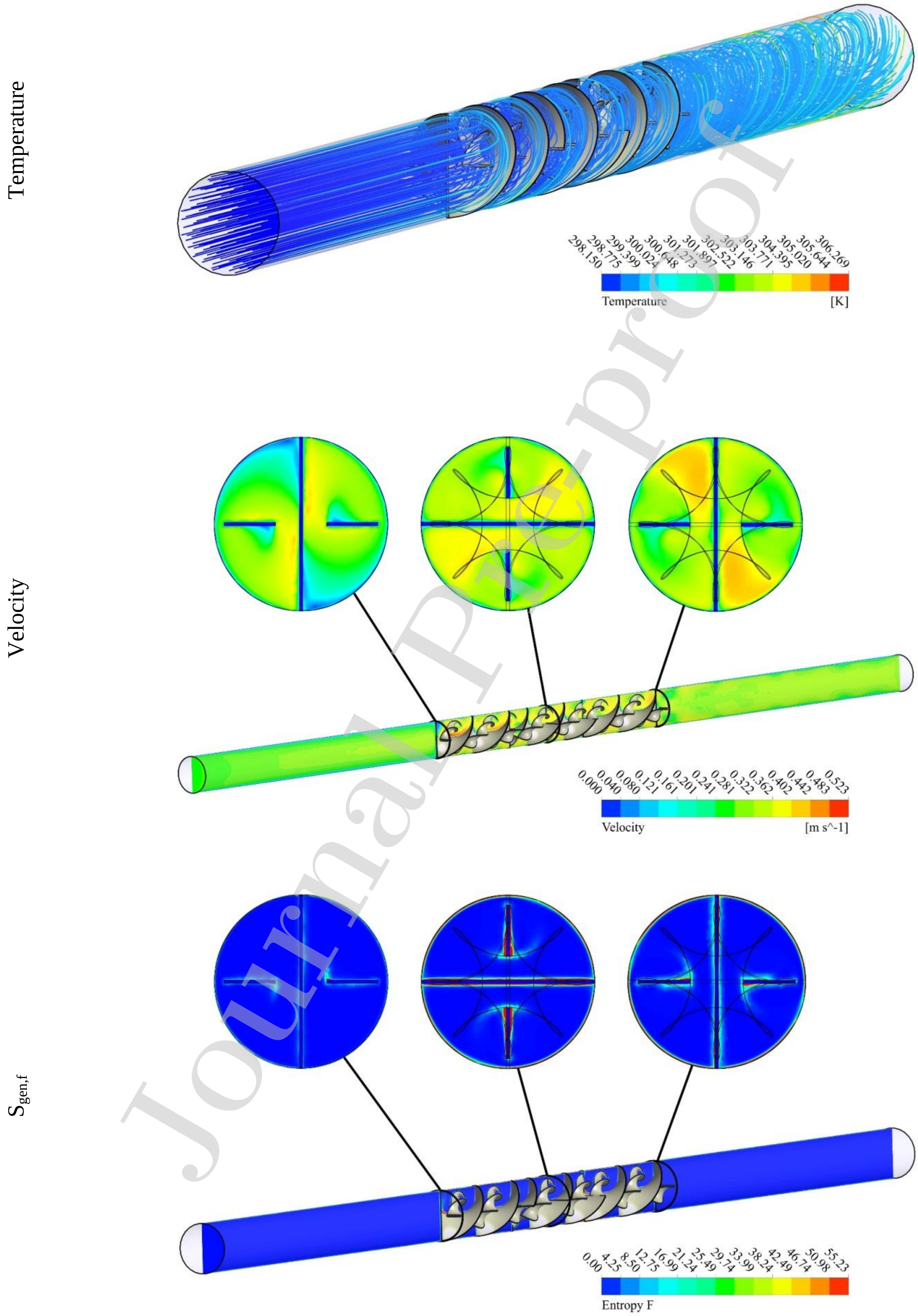
Temperature
298.150
298.775
299.399
300.024
300.648
301.273
301.897
302.522
303.146
303.771
304.395
305.020
305.644
306.269
Temperature
[K]
Velocity
0.000
0.040
0.080
0.121
0.161
0.201
0.241
0.281
0.322
0.362
0.402
0.442
0.483
0.523
Velocity
[m s^-1]
$S_{gen,f}$
0.00
4.25
8.50
12.75
16.99
21.24
25.49
29.74
33.99
38.24
42.49
46.74
50.98
55.23
Entropy F

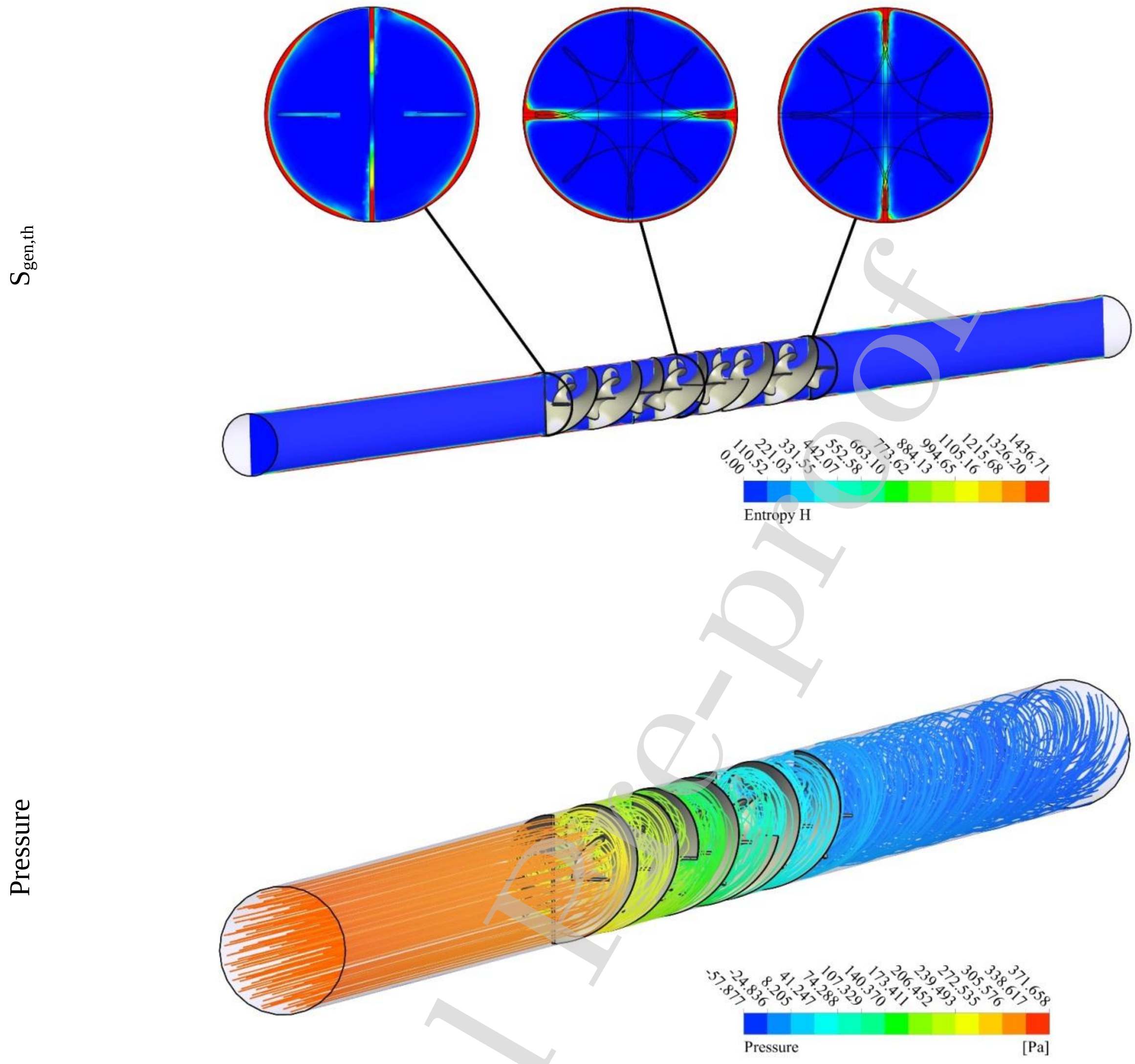

Fig. 8. Velocity, T, P, S_{gen} contours at Re=15000, b=15mm

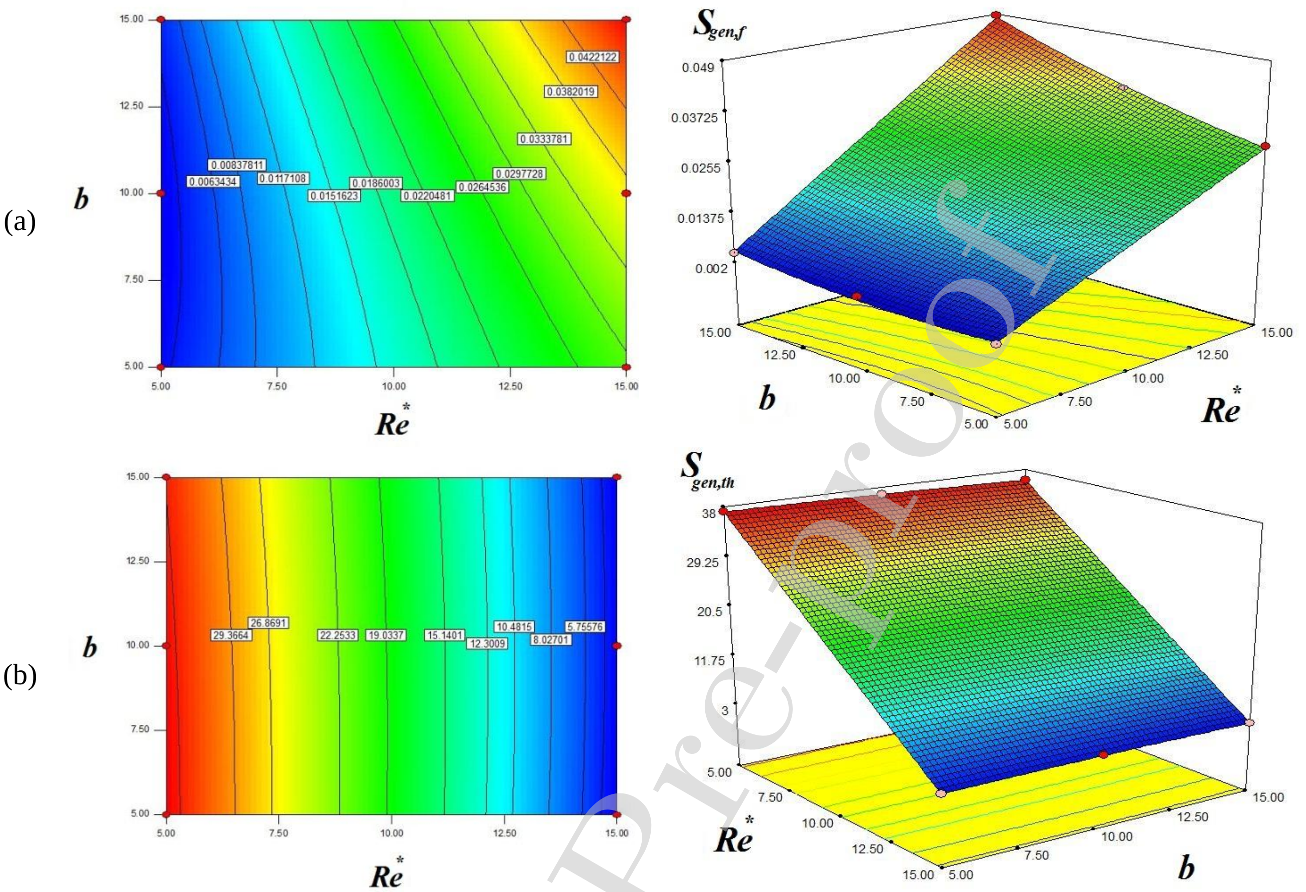

Fig. 9. Components of S_{gen} for various *Re* and *b*.